STRUCTURE AND STATIC AND DYNAMIC MAGNETIC PROPERTIES OF Sr(Co$_x$Ti$_x$)Fe$_{12–2x}$O$_{19}$ HEXAFERRITES PRODUCED BY SELF-PROPAGATING HIGH-TEMPERATURE SYNTHESIS

E. P. Naiden,[1] **V. A. Zhuravlev,**[1] **V. I. Itin,**[2]
R. V. Minin,[2] **V. I. Suslyaev,**[1] **and O. A. Dotsenko**[1]

UDC 538.62, 548:537.611.46

A resource-effective process to synthesize Sr(Co$_x$Ti$_x$)Fe$_{12–2x}$O$_{19}$ *hexaferrites is proposed. The values of saturation magnetization and anisotropy field of the resulting materials are determined. It is shown that an interpretation of the ferromagnetic resonance (FMR) spectra requires that anisotropy of the magneto-mechanical ratio should be taken into account in addition to magnetic anisotropy.*

Keywords: SHS, hexaferrites, ferromagnetic resonance, crystallographic magnetic anisotropy.

Materials based on oxide ferrimagnetics (ferrites) are extensively used in various fields of science and technology, in particular, in radio electronics, electrical engineering, instrument making, etc. Among a variety of ferrites, the most appealing are the hexagonal oxide ferrimagnetics, such as strontium hexaferrite, SrFe$_{12}$O$_{19}$(Sr–M), which possesses high values of the field of crystallographic magnetic anisotropy (CMA) and magnetization and demonstrates a high stability of these characteristics in a wide temperature interval [1, 2]. This ferrimagnetic material and the diamagnetically dilute systems thereof are widely applied as active components of radar-absorbent materials and microwave devices. It should be noted that their maximum electromagnetic energy absorption falls within the range of frequencies of a natural ferromagnetic resonance, which is determined by the anisotropy field and material microstructure – grain size and shape. It is well known that an effective way to improve the structural and magnetic properties of ferrites is to introduce a variety of dopants into the base material, which result in the formation of substituted structures. In the case of strontium hexaferrites, a substitution of Co^{2+}Ti^{4+} for a part of iron Fe^{3+} ions gives rise to a considerable decrease in the value of crystallographic magnetic anisotropy and a shift of the frequency of the natural ferromagnetic resonance and, hence, the service band of effective absorption towards the low-frequency part of the microwave range [3, 4].

Within the recent decades, new, advanced resource-saving processes for manufacturing ferrites have been developed, which rely on the method of self-propagating high-temperature synthesis (SHS) taking place in the mode of filtration combustion of iron powders and those of oxides of other elements in the reacting gas atmosphere: oxygen or air [5,6].

The purpose of this work is to synthesize the M-phase stronzium hexaferrites, Sr(Co$_x$Ti$_x$) Fe$_{12–2x}$O$_{19}$ ($0 \leq x \leq 1.0$), using SHS and to analyze their static and dynamic magnetic properties. In all stages of the process, we determined their phase composition and structure parameters.
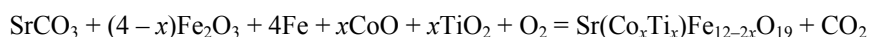
[1] Tomsk State University, Tomsk, Russia, [2] Department of Structural Macrokinetics of the Siberian Branch of the Russian Academy of Sciences, Tomsk, Russia, e-mail: ptica@mail.tsu.ru.

TABLE 1. Phase Composition and Structure Parameters of End Products in a $Sr(Co_xTi_x)Fe_{12-2x}O_{19}$ System Subjected to the Following Pre-treatment: 3 min. MCA + SHS + Ferritization at 1200°C for 2 Hours.

Composition	Sr–M, Vol.%	CSR, nm	$\Delta d/d \cdot 10^3$	Fe_2O_3, Vol.%	CSR, nm	$\Delta d/d \cdot 10^3$
$SrFeO_{19}$	96	120	0.30	4	–	–
$SrCo_{0.5}Ti_{0.5}Fe_{11}O_{19}$	94	60	0.15	6	–	–
$SrCo_{0.6}Ti_{0.6}Fe_{10.8}O_{19}$	94	100	0.60	6	–	–
$SrCo_{0.7}Ti_{0.7}Fe_{10.6}O_{19}$	94	63	1.10	6	–	–
$SrCo_{0.8}Ti_{0.8}Fe_{10.4}O_{19}$	92	72	0.30	8	21	3.5
$SrCo_{0.9}Ti_{0.9}Fe_{10.2}O_{19}$	91	93	0.70	9	–	–
$SrCo_{1.0}Ti_{1.0}Fe_{10}O_{19}$	85	85	0.70	15	103	1.0

SYNTHESIS OF POWDERS AND THEIR X-RAY EXAMINATION

To synthesize the powders, use was made of the following chemical reactions:

$$SrCO_3 + (4 - x)Fe_2O_3 + 4Fe + xCoO + xTiO_2 + O_2 = Sr(Co_xTi_x)Fe_{12-2x}O_{19} + CO_2$$

and the reagents: strontium carbonate, iron oxide Fe_2O_3, cobalt oxide CoO, titanium oxide TiO_2, and R10-grade iron.

In order to promote the rate of conversion during the SHS process, we used mechanochemical pre-activation (MCA) of the reaction mixture in a water-cooled planetary ball mill (WPM). The ball-to-mixture mass ratio used was 20:1, which corresponded to the power density 60 g. The activated mixture of reagents with a porosity of 60–70% was fed into the reactor and ignited. After the SHS process was over, the reaction products were subjected to ferritization in a muffle furnace at the temperature 1200–1250°C for 2 hours in air.

The phase composition and structure parameters of the resulting material were determined in a Shimadzu XRD 6000 x-ray diffractometer (using CuK_α radiation). The x-ray diffraction data were processed using the POWDER CELL 2.5 software. As a result, we identified the phase composition, the size of coherent scattering regions (CSRs), and the value of internal elastic microstresses proportional to the relative interplanar-spacing variations ($\Delta d/d$).

The magnetic measurements included an investigation of magnetization curves in the pulsed magnetic fields and ferromagnetic resonance (FMR) spectra within the frequency range 26–53 GHz. During the FMR analysis, the hexaferrite powders were placed into quartz tubes with an inner diameter of 0.7 mm and length of 10 mm. The powder sample density was the same for all powders and was found to be ≈2.86 g/cm^3. The permeability and permittivity spectra of the synthesized powders were investigated at the frequencies within 3–12 GHz using a universal wideband spectrometer based on an Agilent Technologies vector network analyzer. We applied the resonance method with a set of rectangular cavities used as measuring cells. The hexaferrite powder samples under study were placed into a 2 mm quartz tube. The sample density was monitored by weighing them in a Shimadzu AUX320 electronic balance.

Tables 1 and 2 summarize the x-ray diffraction data obtained from the SHS end products. It is evident that the mechanochemical pre-activation of the initial mixtures gives rise to a significant increase in concentration of the Sr–M master phase up to 75–78% by volume after the SHS process. For the case without any mechanochemical activation, the master phase content after SHS was 60–70% by volume. The average grain size was below 100 nm for all mixture compositions. In addition to the master phase, there are nanosized phases of magnetite and iron oxide α-Fe_2O_3. Their content is found to be 13–25% by volume. A subsequent ferritization in air at 1200°C for 1 hour results in an increase in the content of the master phase, Sr–M, up to as high as 91–96% by volume, while the concentration of α-Fe_2O_3 decreases down to 4–9% by volume, and there are no traces of magnetite in the end product (Table 1). The grain sizes increases but slightly. The blank boxes in the tables denote that this parameter was not estimated.

In order to increase the average grain size, we performed an additional ferritization process at the temperature 1250°C for 2 hours. The results are given in Table 2.

TABLE 2. Phase Composition and Structure Parameters of End Products in a $Sr(Co_xTi_x)Fe_{12-2x}O_{19}$ System Subjected to the Following Pre-treatment: 3 min. MCA + SHS + Ferritization at 1200°C for 2 Hours + Additional Ferritization at 1250°C for 2 Hours.

Composition	Sr–M, Vol.%	CSR, nm	$\Delta d/d \cdot 10^3$	Fe_2O_3, Vol.%	CSR, nm	$\Delta d/d \cdot 10^3$
$SrFeO_{19}$	99	≥ 1000	–	1	–	–
$SrCo_{0.5}Ti_{0.5}Fe_{11}O_{19}$	95	≥ 1000	–	5	–	–
$SrCo_{0.6}Ti_{0.6}Fe_{10.8}O_{19}$	95	≥ 1000	–	5	30	2.2
$SrCo_{0.7}Ti_{0.7}Fe_{10.6}O_{19}$	96	≥ 1000	–	4	–	–
$SrCo_{0.8}Ti_{0.8}Fe_{10.4}O_{19}$	95	≥ 1000	–	5	–	–
$SrCo_{0.9}Ti_{0.9}Fe_{10.2}O_{19}$	91	≥ 1000	–	9	–	–
$SrCo_{1.0}Ti_{1.0}Fe_{10}O_{19}$	88	≥ 1000	–	12	–	–

TABLE 3. Specific Magnetization and Anisotropy Fields of $Sr(Co_xTi_x)Fe_{12-2x}O_{19}$ Hexaferrites

Concentration, x	0.0	0.5	0.6	0.7	0.8	0.9	1.0
M_s, $Gs \cdot cm^3/g$	76.4	74.2	73.8	73.3	72.3	71.6	68.9
H_a, kOe	18.8	17.1	16.2	15.0	13.0	11.5	10.3

According to the data presented in Table 2, an additional ferritization process increases the content of the master phase, Sr–M, and decreases that of α-Fe_2O_3. The grain size significantly increases to over 1 μm, while the elastic microstresses decrease.

Thus, following a two-stage ferritization we have manufactured single-domain uniformly distributed hexaferrite particles of a $Sr(Co_xTi_x)Fe_{12-2x}O_{19}$ system.

INVESTIGATION OF MAGNETIZATION CURVES

An investigation of the magnetic-field dependences of magnetization and its second derivative of the M-type strontium hexaferrite powders doped with $Co^{2+}Ti^{4+}$ was performed in a pulse magnetometer in the fields up to 50 kOe at room temperature. The measured specific magnetization (σ) and the values of anisotropy fields (H_a) of the synthesized materials are presented in Table 3.

Note that the values of magnetization and anisotropy fields for strontium ferrites, including substituted ferrites, are close to the literature data for single crystals [7] and powder specimens produced using conventional ceramic processing techniques [8].

Shown in Figs. 1 and 2 are the temperature dependences of principal magnetic characteristics of strontium hexaferrites with the concentration of $Co^{2+}Ti^{4+}$ ions equal to 1.0.

It is evident that the saturation magnetization for this hexaferrite composition decreases nearly linearly with increasing temperature. In the temperature dependence of the field anisotropy there is a temperature interval from 300 to 500 K, wherein field anisotropy hardly depends on temperature, i.e., this ferrimagnetic is a promising material to build thereon thermally stable radar-absorbing devices and coatings for the range of frequencies $\approx$20–30 GHz.

INVESTIGATION OF MAGNETIC ANISOTROPY OF NANOSTRUCTURED HEXAFERRITE POWDERS OF A $Sr(Co_xTi_x)Fe_{12-2x}O_{19}$ SYSTEM BY THE FMR METHOD

Figure 3 shows the curves of ferromagnetic resonance I obtained from $SrCoTiFe_{10}O_{19}$ hexaferrite powders. The numerals with arrows are the measuring frequencies in GHz. They have a form common for the easy magnetization axis anisotropy (EMA). The resulting spectra were processed using the techniques described in [9].
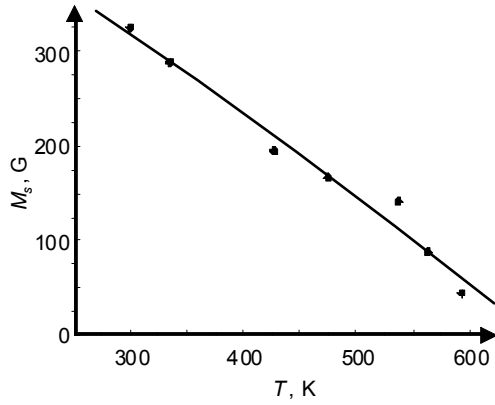
Fig. 1

Fig. 2

Fig. 1. Temperature dependence of saturation magnetization of $Sr(Co_{1.0}Ti_{1.0})Fe_{10}O_{19}$ hexaferrites.
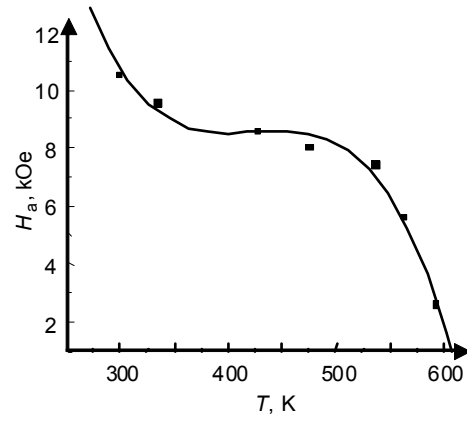
Fig. 2. Temperature dependence of anisotropy field of $SrCo_{1.0}Ti_{1.0}Fe_{10}O_{19}$ hexaferrites.
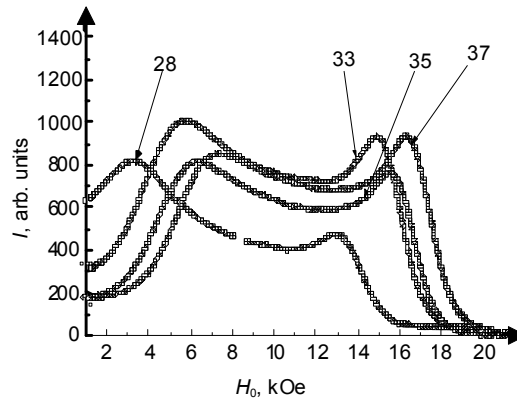

Fig. 3. Resonance curves from $SrCo_{1.0}Ti_{1.0}Fe_{10}O_{19}$ hexaferrite powders.

The FMR curves obtained from the powder specimens contain a number of singularities – maximums and kinks. The low-field singularity corresponds to the resonance of crystallites whose magnetization-field direction is close to the EMA. The high-field singularity corresponds to the resonance of crystallites whose magnetization-field direction is close to the hard magnetization direction (HMD). Within the range of concentrations x under considerations, the EMA is directed along the hexagonal axis of the crystallites, and the HMDs are found in the basal plane that represents a hard magnetization plane (HMP). The resonance field (frequency) values for these directions are determined from the following formula [9]:

$$\omega_{\parallel} = \gamma_{\parallel}\left[H + \frac{\gamma_{\perp}}{\gamma_{\parallel}} H'_{a1} \right], \quad \omega_{\perp} = \gamma_{\perp}\left[H\left(H - H'_{\theta}\right) \right]^{1/2}. \tag{1}$$

Here $\omega_{\parallel}$, $\gamma_{\parallel}$ and $\omega_{\perp}$, $\gamma_{\perp}$ are the resonance frequencies and the magnetomechanical ratio for directions along the hexagonal axis and those in the base plane, respectively, H'_{a1}, H'_{θ} are the fields of magnetic anisotropy for these directions. These fields include the contributions from crystallographic magnetic anisotropy and anisotropy of sample
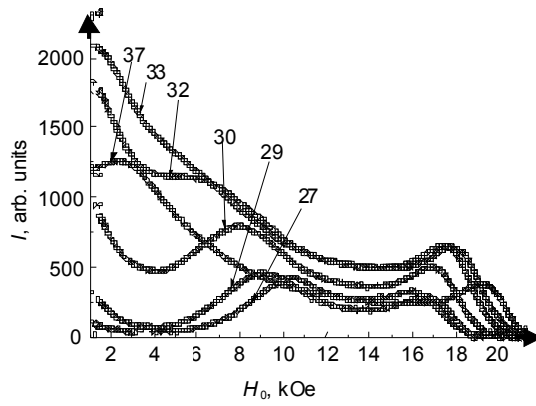
872

Fig. 4. Resonance curves from $SrCo_{0.7}Ti_{0.7}Fe_{10.6}O_{19}$ hexaferrite powders.

shape. With decreasing frequency, the maximums in the FMR curves shift towards lower fields. An increased loss in the zero magnetic fields with decreasing frequency is due to the microwave frequency drawing closer to that of the natural ferromagnetic resonance (NFMR), which is given by

$$\omega_{NFMR} = \gamma_{\perp} H'_{a1} . \tag{2}$$

As the content of CoTi is decreased, starting from $x = 0.8$, an additional maximum appears in the FMR curves within a certain frequency range, depending on the value of x, whose behavior is cardinally different from that calculated via formulas (1).

This is illustrated in Fig. 4, which also presents the resonance curves from the material with $x = 0.7$. The frequency 33 GHz is close to the NFMR frequency (2). At higher frequencies, the behavior of the NFMR spectra is ordinary (see Fig. 3). As the frequency is decreased, additional maximums appear in the resonance curves, which shift towards higher fields, approaching the high-field maximum. This type of oscillations, according to [10], is observed in single-domain particles with the anisotropy of the EMA type for the magnetization field orientation within the HMP and the values of $H_0 \leq H'_\theta$. Note that the magnetization vector is shifted from the HMP ($\theta_0 = \pi/2$) towards the EMA ($\theta_0 = 0$). The equilibrium orientation of the magnetization vector (angle θ_0) and the resonance frequency of this type of oscillations (ω_3) are determined from the formulas
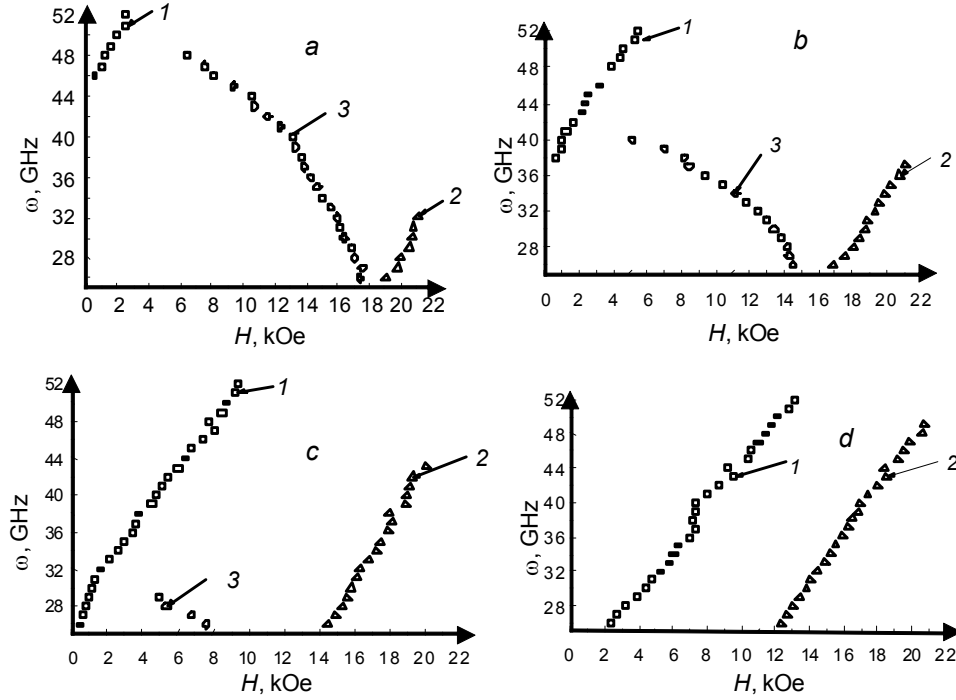
$$\theta_0 = \arcsin(H_0 / H'_{a1}), \ \omega_3 = \gamma_\perp \left[\left(H'_{a1} \right)^2 - H_0^2 \right]^{1/2}, \tag{3}$$

obtained in an assumption that only the first anisotropy constant k_1 plays a significant role in the energy of crystallographic magnetic anisotropy. Shown in Fig. 5 are the experimental dependences of resonance frequencies of a number of specimens investigated in this study. Numeral *1* in the figures indicates the branch of spectrum for the crystallites resonating near the frequency $\omega_{\parallel}$ (EMA), Numeral *2* – $\omega_{\perp}$ (HMP), and Numeral *3* – ω_3. As the concentration of the $Co^{2+}Ti^{4+}$ ions is increased, branches *1* and *2* approach each other, and the point of intersection of branch *1* with the ordinate axis, which corresponds to the frequency ω_{NFMR}, and branch *3* are shifted towards lower frequencies. This behavior results from the decreased value of the anisotropy field.

Note that formulas (1)–(3) were obtained for a single crystal hexaferrite specimen shaped as an ellipsoid of revolution with an axis parallel to the hexagonal axis *c*. The values of resonance fields (or frequencies), which have singularities – maximums and kinks – in the FMR curves from the powder specimens, would coincide with those calculated via these formulas in the case of negligibly small dissipation only [10]. While appro0ximating the

TABLE 4. Magnetomechanical Ratios of Hexaferrites of a $Sr(Co_xTi_x)Fe_{12-2x}O_{19}$ System

Concentration, x	$\gamma_\parallel$, GHz/kOe	$\gamma_\perp$, GHz/kOe	$\Delta\gamma = \gamma_\perp - \gamma_\parallel$, GHz/kOe	$\omega_{NFMR}/2\pi$, GHz
0.0	2.90 ± 0.10	2.90 ± 0.20	0.00 ± 0.30	44 ± 4
0.5	2.75 ± 0.08	2.70 ± 0.06	0.00 ± 0.10	37 ± 2
0.6	2.59 ± 0.08	2.87 ± 0.06	0.30 ± 0.10	35 ± 2
0.7	2.54 ± 0.07	3.00 ± 0.08	0.50 ± 0.20	31 ± 2
0.8	2.51 ± 0.04	2.94 ± 0.05	0.43 ± 0.09	28 ± 1
0.9	2.59 ± 0.03	2.85 ± 0.04	0.26 ± 0.07	23 ± 1
1.0	2.51 ± 0.04	2.72 ± 0.03	0.21 ± 0.07	19 ± 1

Fig. 5. FMR spectra from the specimens under study for different concentrations: $x = 0.0$ (*a*), 0.5 (*b*), 0.8 (*c*), and 1.0 (*d*). Their interpretation is given in the text.

experimental dependences of branches 1 and 2 using formulas (1) from the tilt of the $\omega(H)$ plot, we estimated only the values of magnetomechanical ratios $\gamma_\parallel$ and $\gamma_\perp$. The resulting data are summarized in Table 4.

According to Table 4, substitution of part of iron ions with the $Co^{2+}Ti^{4+}$ complex gives rise to an appreciable anisotropy of the magnetomechanical ratio $\Delta\gamma$, with this anisotropy nonmonotonically depending on concentration, reaching its maximum near $x = 0.7$ (Fig. 6). An extrapolation of the experimental data for the ω branch of the FMR spectrum towards the zero magnetization fields allows us to evaluate the NFMR frequencies ω_{NFMR} for the materials under study. The data are presented in the last column of Table 4. It is evident that an increase in the concentration of $Co^{2+}Ti^{4+}$ ions from zero to unity gives rise to a nearly twofold decrease in the NFMR frequency.

The values of the anisotropy fields H'_{a1} and H'_θ were estimated via a detailed comparison of the experimental and calculated FMR plots [9]. The results of these estimations are presented in Table 5. The bottom row of Table 5 lists the concentration dependences of the contribution from higher-order anisotropy constatnts derived using the following formula: $H_{a2} + H_{a3} = H'_\theta - H'_{a1}$, the error being ± 0.2 kOe.

TABLE 5. Anisotropy Fields of $Sr(Co_xTi_x)Fe_{12-2x}O_{19}$ Hexaferrites

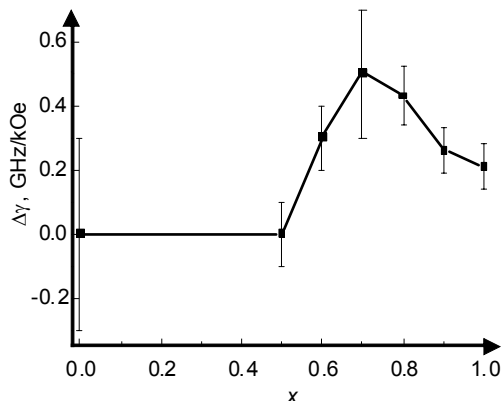| x	0.0	0.5	0.6	0.7	0.8	0.9	1.0
H'_{a1}, kOe	16.4	15.2	13.5	12.3	10.5	9.7	8.4
$H_{a2} + H_{a3}$, kOe	–	–	–	–	0	–1.2	–2.4

Fig. 6. Concentration dependence of anisotropy of magnitomechanical ratio $\Delta\gamma = \gamma_{\perp} - \gamma_{\parallel}$ of $Sr(Co_xTi_x)Fe_{12-2x}O_{19}$ hexaferrites.

A comparison of the measured values of the anisotropy fields H'_{a1} with the static measurements summarized in Table 3 imply that static measurements provide larger anisotropy fields for all compositions in question. This might be related both to the differences in the measurement techniques used (e.g., different contributions from demagnetizing fields of the grains and the specimen into the total magnetic anisotropy field) and special features of the FMR in materials with an anisotropic gyromagnetic ratio [11]. From practical measurements of the FMR, it is anisotropy of mechanical rather than magnetic moment, which is determined in such materials. The influence of the second- and third order anisotropy constants increases with the content of the $Co^{2+}Ti^{4+}$ ions.

DYNAMIC CHARACTERISTICS OF $Sr(Co_xTi_x)Fe_{12-2x}O_{19}$ HEXAFERRITES

Dynamic properties of hexaferrite powders were investigated by the resonance-frequency method [12]. The spectra of permeability ($\mu = \mu' - i\mu''$) and permittivity ($\varepsilon = \varepsilon' - i\varepsilon''$) from the powders of strontium hexaferrite are presented in Figs. 7 and 8. It is clear that the real part of permeability is close to unity and the imaginary part is small in this part of the frequency range, since the frequencies of the natural ferromagnetic resonance for this material lie at $\approx$44GHz. The dielectric losses are also small. The dynamics of variations in the real part of permeability with increased concentration of the $Co^{2+}Ti^{4+}$ ions is given in Fig. 9. Since with increasing x the NFMR frequency is decreased down to 19 GHz. ($x = 1.0$), there is a slight increase in the real part of permeability. The measured values of imaginary permeability are below 0.1. Permittivity of the powders within the range of concentrations $0.5 \leq x \leq 1.0$ undergoes no variations and is found to be $\varepsilon = 5.7 - i0.3$.

Thus, it has been shown that the method of self-propagating high-temperature synthesis combined with a preliminary mechanical-chemical treatment and final ferritization allows one to produce single-domain strontium ferrite powders. Based on this method, we have proposed several resource-saving processes for manufacture of complex strontium hexaferrites, which offer an advantage of fewer production operations and a lower cost compared to the ceramic manufacturing procedure. It has been shown that in order to ensure a correct interpretation of dynamic properties of $Sr(Co_xTi_x)Fe_{12-2x}O_{19}$ hexaferrites, one has to take into account anisotropy of the magnetomechanical ratio
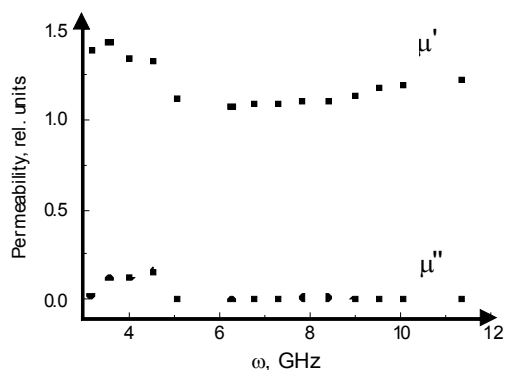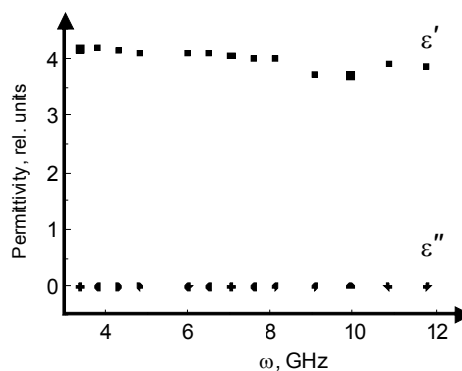
Fig. 7. Permeability spectra from $SrFe_{12}O_{19}$ hexaferrite.

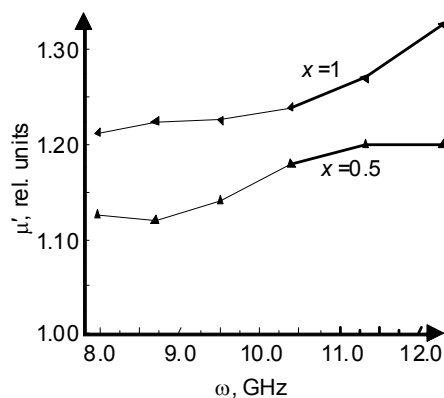Fig. 8. Permittivity spectra from $SrFe_{12}O_{19}$ hexaferrite.

Fig. 9. Spectrum of the real part of permeability of $Sr(Co_xTi_x)Fe_{12-2x}O_{19}$ hexaferrites.

in addition to crystallographic magnetic anisotropy. As the content of $Co^{2+}Ti^{4+}$ is increased, the role of the higher-order anisotropy constants becomes more marked. An analysis of the FMR data and the investigations of anisotropy of the above material in pulsed magnetic fields have demonstrated that the resulting hexaferrites synthesized within the range of concentrations $x = 0.0–1.0$ are quite promising in terms of their application in designing radar-absorbing devices and coatings operating in the range 20–50 GHz.

REFERENCES

1. J. Smith and H. Wein, Ferrites [Russian translation], IL (1958).
2. B. Wartenberg, Z. Angew. Phys., **24**, 211 (1968).
3. H. Severin and J. P. Stoll, Z. Angew. Phys., **23**, No.3, 209 (1967).
4. Han-Shin Cho and Sung-Soo Kim, IEEE Magn., **35**, 3151 (1999).
5. A. V. Komarov, P. B. Avakyan, and M. D. Nersesyan, Zh. Fiz.Gor.Vzr., No. 5, 51–56 (1993).
6. A. V. Komarov, V. D. Nersesyan, P. B. Avakyan, and A. G. Merzhanov, Int. J. SHS, **2**, No.3, 239–246 (1993).
7. A. D. Schurova, T. M. Perekalina, and V. P. Cheparin, Zh. Eksp. Teor. Fiz., **55**, Issue 4(10), 1197–1203 (1968).
8. H. Kojiama Ferromagnetic Materials. Chapter 5. Fundamental Properties of Hexagonal Ferrites with Magnetoplumbite Structure (Ed. E.P. Vohlfarth), North-Holland Publ. Co. (1982).

9. V. A. Zhuravlev, Fiz. Tverd. Tela, **41**, No. 6 (1999).
10. A. G. Gurevich, Magentic Resonance in Ferrites and Antiferromagnetic Materials [in Russian], Moscow, Nauka (1973).
11. K. B. Vlasov and B. Kh. Ishmukhametov, Fiz. Met. Metalloved., Issue 1, No. 1 (1961).
12. E. P. Naiden, V. I. Suslyaev, A. V. Bir, and M. V. Politov, Zh. Strukt. Khim., **45**, 102–105 (2004).